EasyChair Preprint

№ 4780

Examination on the processes of structural performance evaluation of SRC deep beams by FEA with NDT results

Motonori Yasui, Pengru Deng and Takashi Matsumoto

December 23, 2020

Examination on the processes of structural performance evaluation of SRC deep beams by FEA with NDT results

Motonori Yasui[1*], *Deng* Pengru[2] and *Takashi* Matsumoto[2]

[1]Hokkaido University, Graduate School of Engineering, Kita 13 Nishi 8, Kita-ku, Sapporo, Japan
[2]Hokkaido University, Faculty of Engineering, Kita 13 Nishi 8, Kita-ku, Sapporo, Japan

* Corresponding author. Tel: +81-11-706-6172; fax: +81-11-706-6172
E-mail address: motonori@eis.hokudai.ac.jp

Abstract. Maintenance of bridges is becoming increasingly important in Japan. In the maintenance of bridges, it is necessary to evaluate the current load carrying capacity of a deteriorated structure by the use of design equations or numerical analyses. However, the design drawings are often missing, thereby input parameters such as material properties and internal reinforcement arrangements for the equations and analyses are not available. In such a case, it is necessary and important to determine the input parameters by destructive or non-destructive tests (NDT) or rational judgements and to estimate the load carrying capacity of a deteriorated structure with a rational analytical model. In this study, using NDT results, the structural performance of SRC deep beams is evaluated by FEA, where the evaluation processes are examined as well. Considering that the material properties from NDT has some ranges and may contain errors, their values are adjusted referencing the design of similar beams from some papers and then input for FEA. In terms of concrete, a nonlinear stress-strain relation is employed for compression. Under tension, the concrete is assumed to behave linear elastically before the tensile strength is reached. After that, a linear softening behavior is assumed for cracked concrete. As for steel reinforcements, i.e. embedded I-beam and rebars, the stress-strain relation is assumed as elastoplastic. The steel/concrete interface is regarded as rigidly connected. In addition to FEA, hand calculation using empirical equations is conduced as well to examine the predictions. Finally, the predictions such as internal structure, material properties and load carrying capacity are compared with their corresponding experimental results which have been closed until this step. From this comparison, the employed performance evaluation processes are examined.

Keywords: maintenance, structural performance evaluation, SRC, deep beam, FEA, NDT.

1 Introduction

Nowadays, existing bridges are required to be inspected once every five years. In Japan, the number of infrastructures which are over 50 years old is increasing. It is reported by the Ministry of Land, Infrastructure, Transport and Tourism of Japan that the ratio occupied by such structures will be 60% in the upcoming 20 years [1]. Therefore, it is of great importance to provide effective maintenance and evaluation for those structures.

Unfortunately, the design drawings are lost for some existing structures. Thus, to evaluate the performance of these structures, one has to obtain or estimate the values of the material properties and the structural type and arrangement of the internal structures including concrete, reinforcement rebar and members based on destructive or non-destructive tests or rational predictions. Even though the structural performance can be evaluated easily using appearances such as the degree of cracking, the evaluations are rather rough and the reliability of these evaluations can hardly be checked and verified. However, theoretically, as the status of an existing structure can be reflected on some structural characteristics including the geometrical dimensions, material properties and behaviors under some given loads, a more mechanical sound and accurate performance evaluation can be provided by inputting the data from in-situ inspection, measurement and NDTs into a numerical model of the structures and then conducting analysis. So far, the process of these prediction and evaluation has not been established yet. Nowadays, the process depends on the judgment skill of engineers.

As one of the evaluation methods for such structures, “Blind Performance Evaluation” is currently under consideration at the Committee on Hybrid Structures, Japan Society of Civil Engineers. We also decided to work on blind performance evaluation. The Blind Performance Evaluation is to predict the internal structure of the structure from the data obtained by inspection and measurement of the structure with unknown internal structure, and then evaluate the structure performance including future behavior. Blind performance evaluation has 4 steps. The first step is inspection and measurement. The second step is prediction and analysis of the structure from data of first step. The third step is evaluating the structure. The forth step is comparing the prediction and the experimental results of the actual specimen. Therefore, the performance of an SRC beam is evaluated with the developed method as well as hand calculation using empirical equations. At the meanwhile, the process of structural performance evaluation by conducting FEA of the structure predicted with date from NDTs is examined, which is the primary purpose of this research.

2 The procedure of Blind Performance Evaluation

As shown in section 1, the blind performance evaluation has 4 steps. The first is inspection and measurement. In this study, this step contains two phases. The first phase is only inspection of the structure, such as dimensions and cracking procedure during loading experiment. The second phase is measurement by non-destruction testing

(NDT) techniques. The data obtained from NDT includes the prediction of material property and internal structure arrangement. The second step is prediction and analysis the structure. From the data of first step, the specimen is predicted referring other papers of which specimen is close to this study to determine material property and internal structure arrangement. Then, following this prediction, the analysis is conducted using hand calculation and FEA by MSC/MARC. In this analysis, the behavior is analyzed, such as procedure of cracking, failure mode and the maximum load capacity. The third step is evaluation. In this step, the future behavior of the specimen after damaged is evaluated from data of first step and prediction and analysis of second step. The forth step is comparison the prediction and actual structure and loading experiment.

3 The data from inspection and measurement

The inspection and measurement has 2 phases. The first phase of inspection and measurement is to get only specimen dimensions. Fig.1 shows the geometric information of the specimen. As the reinforcement condition is not available from these information, one can only suppose the specimen as a regular reinforced concrete (RC) beam as this structural type is most commonly employed. The second phase of inspection and measurement is to conduct non-destruction test (NDT) to get material property and internal steel arrangement. The arrangement of internal structure determined from NDT is shown in Fig.1. In terms of the NDT, a microwave radar was used for prediction of steel arrangement and a hammer test was adopted for determining the range of compressive strength of concrete. It is found that the tested specimen may be a steel reinforced concrete beam rather than a normal reinforced concrete beam. Table 1 and Table 2 show ranges of material properties of concrete and steels from NDTs. To investigate the dependence of the accuracy of the proposed method on the completeness and richness of the data from inspection and measurement, prediction of the specimen details is conducted after each phase. The specimen is named as first prediction from the data of the first phase. The specimen is named as second prediction from the data of the second phase.

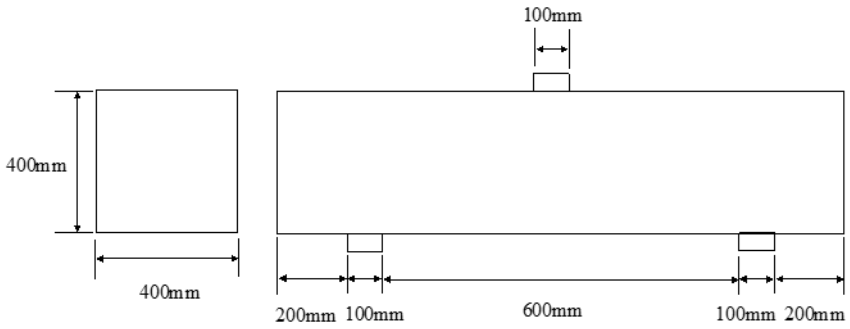

Fig.1 The data of size of specimen

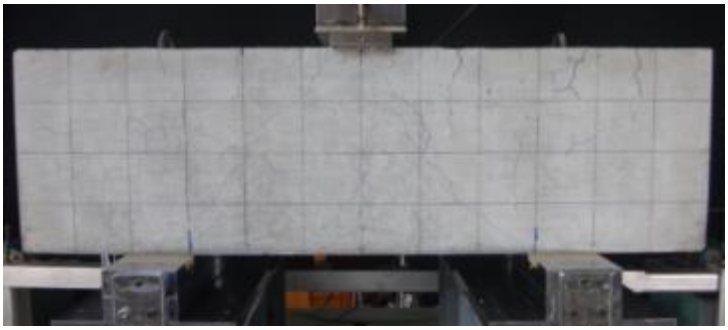

Fig.2 The picture of specimen after cracking

Table 1 The data of concrete from NDT

Compressive strength	26.8 ~ 40.7 MPa
Tensile strength	2.06 ~ 2.72 MPa
Young's modulus	26.4 ~ 31.1 GPa

Table 2 The data of steels from NDT

Diameter of rebar in compressive zone	D16 or D19
Diameter of rebar in tensile zone	D19 or D22
Diameter of stirrups	D13, D16 or D19

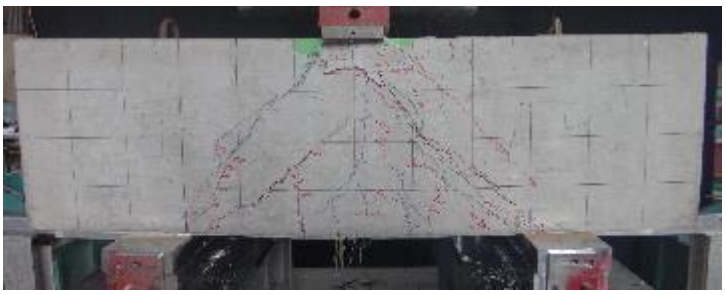

Fig.3 Picture of specimen after failure

4 Prediction of Material Properties and Internal Arrangements

In this study, the paper written by Muhammad SAFDAR [2] is referenced, where a non-linear analysis software MSC/Marc was used to analyze RC beams and slabs repaired with Ultra-high performance fiber reinforced concrete (UHPFRC). In this paper, the same software, MSC/Marc, is used as well. In SAFDAR's paper, it is

showed that the method developed in MSC/Marc can provide an accurate prediction of behaviors including load-displacement of mid-span curve of the tested structures compared to experiment. Therefore, the same theories adopted in SAFDAR's paper are adopted in this study as well.

4.1 Concrete

In this study, two assumptions are employed on the material properties of concrete. The first assumption is that concrete is homogenous and initially isotropic. The second assumption is that the uniaxial compressive stress-strain relationship for the concrete model shown in Fig.4 is obtainable following the multi-linear equations for concrete proposed by MacGegor 1992 [3].

According to first phase of data, i.e. the dimensions of specimen, no information about the concrete was provided. The material properties have to be predicted based on experiences and existing related knowledge, such the design specifications, standard design cases, as the specimen should satisfy the requirements of the design specification and should not be too special. Then two papers were referenced [4][5]. The dimensions of the specimens which were used on these two papers were close to the specimen which are used in this research. From these two papers, it is showed that the maximum compressive strength and Young's modulus of the concrete, f'_c, and, E_c, are close to 30 MPa and 28 GPa. Therefore, in this research, 30MPa and 28GPa were adopted for the compression strength and Young's modulus of the concrete of the specimen named as the first prediction.

According to the second phase of data, it was found that the uniaxial compressive strength and Young's modulus of concrete vary in 26.8 ~ 40.7MPa and 26.4 ~ 31.1GPa, respectively, as shown in Table 1. These ranges include the values, which are predicted at first phase. Under uniaxial compression, the concrete strain, ε_o, corresponding to the peak stress, f'_c , is assumed as 0.002 which is commonly used. The crushing strain, ε_{cu}, of concrete is defined as 0.003 as suggested by ACI committee 318. The Poisson's ratio of concrete is assumed to be 0.2. In terms of the tensile properties of concrete, it is generally accepted that the uniaxial tensile strength, f_t, varies from 2.06 MPa to 2.72 MPa. In this study, the tensile strength is calculated based on equation (5) using the compression strength. Under tension, a linear elastic relation is used for the stress and strain of concrete before cracking, i.e. until the tensile strength of concrete, f_t, is reached. Once the cracking of concrete takes place, a discrete model is used to represent the macro cracking behavior. It is known that cracked concrete of RC member can still carry the tensile stress in the direction normal to the crack, which is known as tension stiffening [6]. In this study, a linear softening model as shown in Fig.5 is adopted to capture the tension-stiffening phenomenon. The softening modulus, E_t, is selected as 2.55 GPa and corresponding strain, ε^*, at which tension stiffening stress reduces to zero is 0.001. During the post-cracking stage, the cracked concrete can still transfer the shear forces through aggregate interlocking or shear friction, which is termed as shear retention. The shear retention is modeled by introducing the shear retention factor, which is an input parameter to reduce the shear modulus after cracking. Numerous analytical results have demonstrated that shear

retention factor has value between 0 and 1 [7]. The shear retention factor is selected as 0.4 in this analysis.

$$f_c = \varepsilon E_c \qquad 0 \le \varepsilon \le \varepsilon_1 \tag{1}$$

$$f_c = \frac{\varepsilon E_c}{1 + \left(\frac{\varepsilon}{\varepsilon_o}\right)^2} \qquad \varepsilon_1 \le \varepsilon \le \varepsilon_o \tag{2}$$

$$f_c = f_c' \qquad \varepsilon_o \le \varepsilon \le \varepsilon_{cu} \tag{3}$$

$$\varepsilon_o = \frac{2f_c'}{E_c} \tag{4}$$

$$f_t = 0.23(f_c')^{2/3} \tag{5}$$

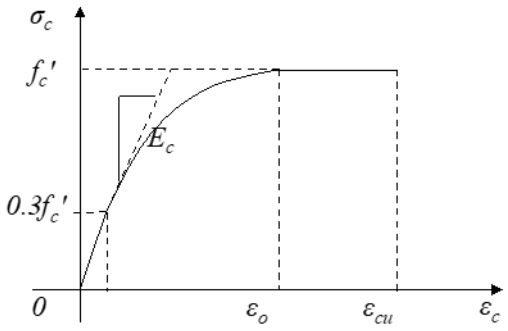

Fig.4 Uniaxial compressive stress-strain curve for concrete

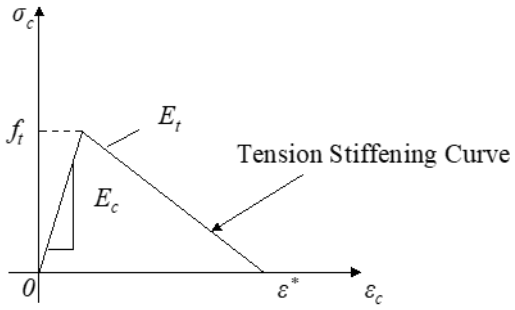

Fig.5 Tension stiffening model for concrete

4.2 Reinforcing Rebar

On first phase of data, any information of internal structure was not given. On second phase of data, material properties of steel include only prediction of range of diameter, no maximum tensile strength, f_{tu}, and yield strength, f_y, and stress-strain curve. Thus, these material properties were predicted according to normal design. Fig.6 shows the constitutive law of reinforcing bar and I-Beam. In this research, a linear elasticity is used for $0 \leq \sigma_s \leq f_y$, and a linear hardening elastoplastic model is applied until a specified ultimate strain is reached under tension and compression. The yield strength and ultimate strength of all reinforcing bar are provided with 345 MPa and 545 MPa respectively. These values are from construction criteria of steel. The ultimate strain ε_u used in this study is 240000 μ. The Poisson's ratio and elastic modulus, E_s, of 0.3 and 200 GPa for both steels are used in this study considering that these values are generally used. Diameter of each reinforcing bar is determined to ensure that the steel ratio of the specimens in this study is similar to the steel ratios used in KOSA's and TANIMURA's papers [4, 5] because the specimens in these papers possess dimensions and material properties approximate to the data from the inspections and measurement in this study. In these papers, the steel ratio of the specimen is 2% in tensile zone and 0.4% in shear zone at the first phase. The diameter of rebar in compressive zone is not important because the rebars in compressive are exploited to facilitate the installation of the stirrups and the compressive stress of rebar is quite small compared to the concrete which has much larger area. According to the above considerations, the diameter of rebars in compressive zone, tensile zone and stirrups are finally determined as D13, D29 and D10 respectively at the first prediction as shown in Fig.7. However, at the second prediction, it is found that these steel ratios are not included in the data of NDTs. Thus, diameters which can provide steel ratios approximate to 2% and 4% were adopted. Finally, at the second prediction, the diameter of rebar in compressive zone, tensile zone and stirrups are determined as D13, D29 and D10 respectively as show in Fig.8. Table 3 shows the determined diameters of each rebar.

4.3 I-beam

At the first prediction, the specimen is predicted as a simple RC beam as no internal information was available after the first phase and the RC beam is the most widely employed structural type. However, it is revealed that the specimen has a steel I-beam as internal reinforcement according to the data of NDT. The beam may be a steel-reinforced concrete (SRC) beam. In a relevant paper presented by MURATA [9], it is found that the yield strength,f_y, of the steel I-beams may vary over a wide range, from 271.6 to 527.6. In this paper, the yield strength of the I-beam of the specimen which is close to the specimen of this research was 351.2 MPa. It is close to the value of rebars, i.e. 345 MPa. In that paper, as no information of other material properties, such as young's modules and maximum tensile strength are available, the material properties of the steel rebar are exploited for the steel I-beam as well for the SRC beam.

4.4 Discussion

Fig.7 and 8 show the first prediction and second prediction, respectively, following sections 4.2 and 4.3. In this chapter, i.e. chapter 4, material properties and internal arrangement are predicted. From only picture of cracking and size, it is too difficult to predict internal arrangement with confidence. Actually, the specimen is predicted as RC beam at the first phase, but it is revealed that the specimen is SRC from NDT at the second phase. Therefore, it is quite important to conduct NDTs for predict internal arrangement and the accuracy of the prediction depend greatly on the richness and completeness of the data from NDTs. With the predicted structural type and material properties, a finite element model of the tested specimen will be developed in chapter 5 to predict the maximum load capacity and also check the influences of NDT on the accuracy of the method.

Table 3 Diameter of rebar

	Rebar of compressive	Rebar of tensile	Stirrups
First prediction	D13	D29	D10
Second prediction	D22	D22	D13

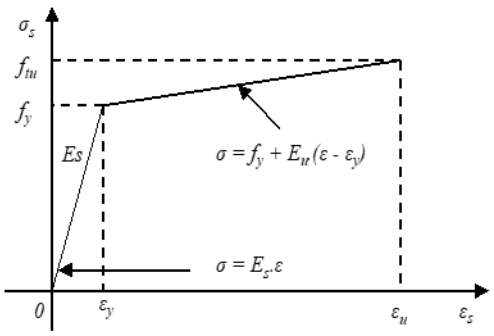

Fig.6 Stress-strain model for steel

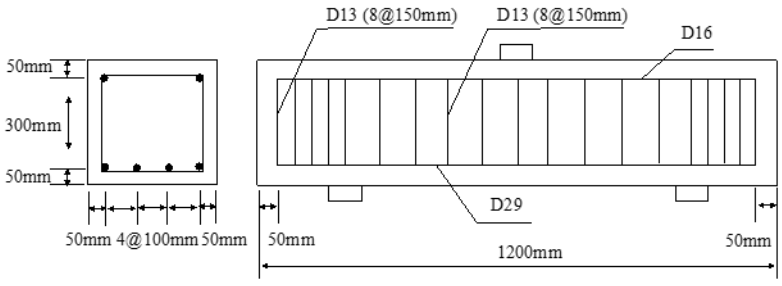

Fig.7 First prediction

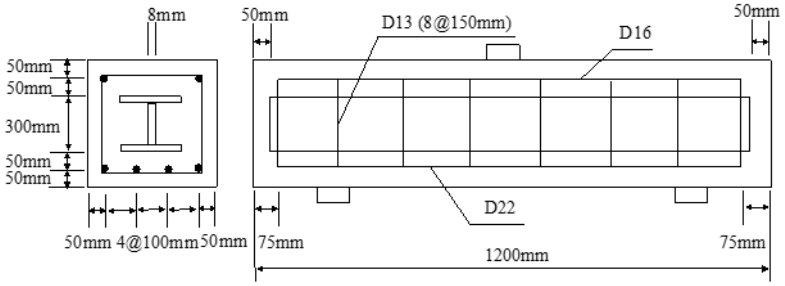

Fig.8 Second prediction

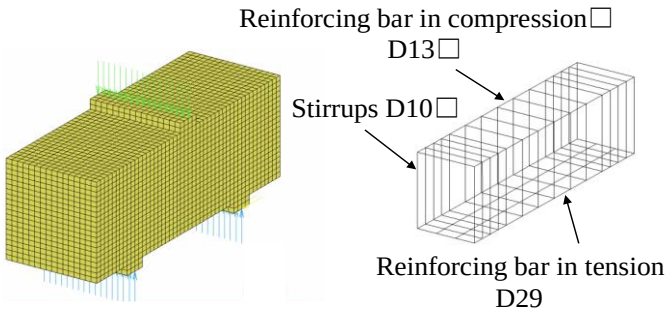

Fig.9 Boundary conditions, mesh and internal arrangement at first prediction

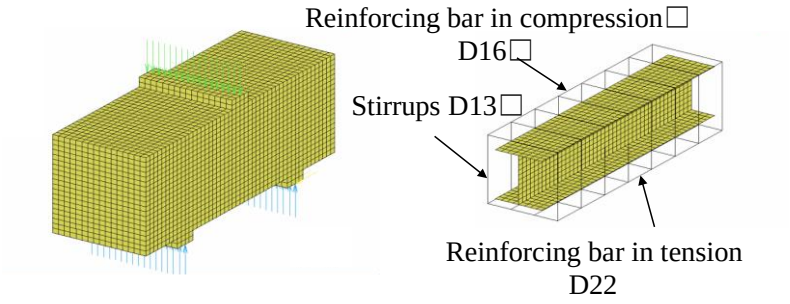

Fig.10 Boundary conditions, mesh and internal arrangement at second prediction

5 Analysis of the predicted structure

5.1 FEA

Finite element analysis is performed by using a nonlinear FEA software, i.e. MSC/Marc. The steel reinforcement is idealized using truss elements with the node points defined such that each rebar element is sharing common nodes with the concrete solids. This approach is called discrete idealization of rebar with concrete. Fig.9 and Fig.10 shows analysis model on MSC/Marc on each prediction phase. Fig.11 shows load–displacement of mid-span curves by FEA of each prediction. It is found that the maximum load capacities are 1003kN and 1593 kN for the first and second predicted specimens, respectively. From FEA, it is generally recognized that the shear failure is difficult to be reproduced output. However, according to TANIMURA's paper [5], the procedure of cracking can be reproduced. In this study, to facilitate the investigation of the cracking procedure, it is defined that a major crack forms once the strain exceeds ε^*, i.e. 0.001, (see Fig. 5). Besides, the shear failure would be defined as once the major shear crack determined according to the definition reaches from bottom side to top side as shown in Fig.12(f) and Fig.13(f), where the gray zones indicate the concrete with tensile strain larger than 0.001.

From the analysis of the first prediction, it is found that the simple RC beam cannot reproduce the procedure of cracking. The cracking process of the first prediction can be divided into 4 steps as follows. Step 1: one flexural crack initiates in tensile zone. Step 2: two flexural cracks initiate adjacent to the crack initiated in step 1 in the tensile zone. Step 3: those two cracks expand to the direction of shear cracking. Step 4: those two shear cracks reach both of the bottom and top sides. And then the shear failure happens according to the definition.

In terms of the analysis of the second prediction, it is found that the procedure of cracking is successfully reproduced by the SRC beam. The cracking process of the second prediction can be divided into 4 steps as follows. Step 1: two flexural cracks initiate in tensile zone. Step 2: two cracks initiate adjacent to the two initiated flexural cracks in step 1. Step 3: these two cracks expands to the direction of shear cracking. Step 4: these two shear cracks reach both of bottom side and top side. And then, the shear failure happens according to the definition in this research. Fig.11 shows the load- displacement curve of the speciemen at mid span.

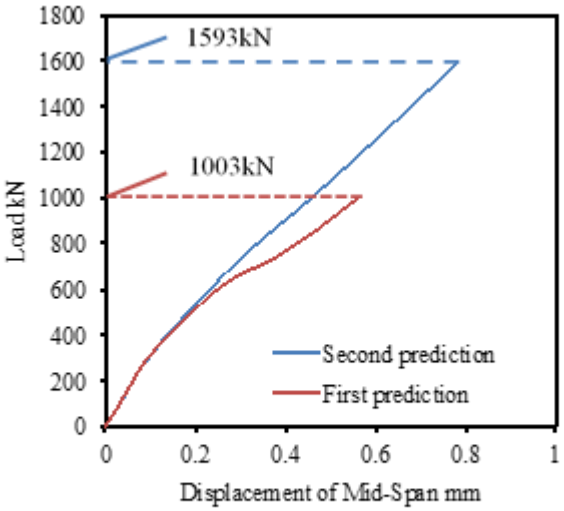

Fig.11 Load-Displacement relation of the specimens at mid-span from FEA

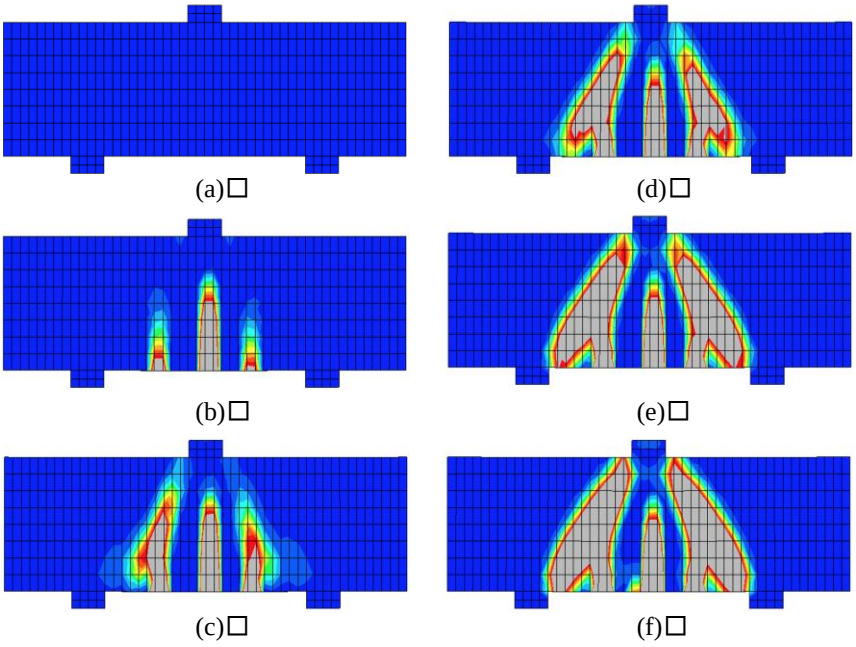

Fig.12 Maximum principal strain of first prediction on Marc

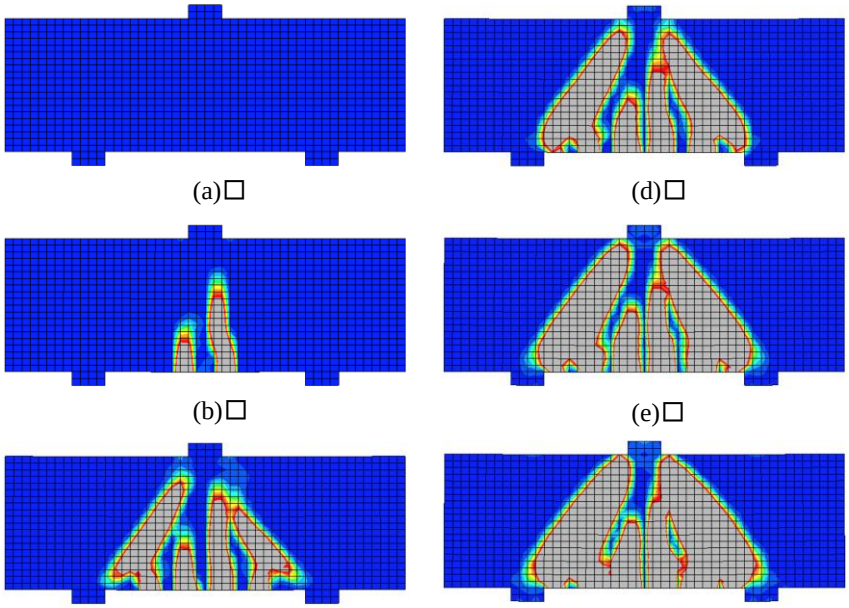

Fig.13 Maximum principal strain of second prediction on Marc

5.2 Hand Calculation

In this research, the hand calculation using empirical equations was conducted for prediction the maximum load capacity and cross check with the results from FEA. In these equations, the assumption is adopted that the maximum load capacity is a summation of the load capacity of each material, such as concrete, stirrups and I-beam. Table 4 shows the calculation result of the first prediction and the second prediction.

$$V_{cal1} = \frac{0.24 f'_c \left(1 + \sqrt{100 p_t}\right) \cdot (1 + 3.33\, r/d)}{1 + (a/d)} b_w \cdot d \tag{6}$$

where, V_{cal1} is the load capacity of RC without stirrups (N). f'_c is compressive strength of concrete (N/mm^2). p_t is the steel ratio in tensile zone. d is the effective height (mm). b_w is the width (mm). r is the length of loading plate (mm). a is the shear span.

$$V_{cal2} = V_{cal1} + \varphi \cdot V_s \tag{7}$$

$$\varphi = -0.17 + 0.3\, a/d + 0.33/(100 p_w) \tag{8}$$

$$V_s = A_w \cdot f_{wy} \cdot Z/S_s \tag{9}$$

where, V_{cal2} is the load capacity of RC with stirrups (N). V_s is the load capacity of stirrups (N). p_w is $A_w/(b \cdot S_s)$. A_w is the amount of area of stirrups in S_s (mm^2). f_{wy} is the yield strength of stirrups (N/mm^2). S_s is the interval of stirrups (mm). Z is d/1.15.

$$V_{cal3} = V_{cal2} + V_{sy} \quad (10)$$

$$V_{sy} = f_{vy} \cdot t_w \cdot Z_w \quad (11)$$

where, V_{cal3} is the load capacity of SRC (N). V_{sy} is the load capacity of I - Beam (N). f_{vy} is the yield strength of I - Beam (N/mm^2). t_w is the thickness of I – Beam (mm). Z_w is the height of I - Beam (mm).

5.3 Discussion of prediction of behavior on loading experiment.

Table 4 shows the result of prediction of load capacity by FEA and hand calculation. As the first prediction shown, the results from FEA and hand calculation are close to each other. From these results, if the prediction of first step of the specimen is correct, the results would be close to the experimental results. However, as the actual specimen is an SRC beam, the results of the specimen from the first prediction should not be close to the experimental results. As shown in the results of the second prediction, the gap between FEA and hand calculation is relatively large. This may be due to the setting of node at FEA. As shown in section 5.1, in this analysis, the rigid connection is adopted. This is considered as a reason of gap of prediction of maximum load capacity of the specimen. On the real specimen, the slip between I-beam structure and concrete happens. However, in this analysis, the slip is ignored. As comparison of first prediction shows, without I-beam, the gap of prediction of maximum load capacity is much larger. Therefore, the connection of concrete and rebar may not have a remarkable effect compared to the connection of concrete and steel I-beam. As a future work, the connection between I-beam structure and concrete may have to be deliberated.

Table 4 Maximum load capacity by FEA and hand calculation

	FEA	Hand calculation
First prediction	1003 kN	957 kN
Second prediction	1593 kN	1298 kN

6 Comparison of Prediction and Actual Specimen

6.1 Arrangement of internal structure

Fig.14 shows the actual design drawing of the specimen. Comparing the second prediction, the steel arrangement is similar to the actual design drawing. The difference of the second prediction and the actual design is the rebar diameters and the length of steel I-Beam. Table 5 shows the actual diameter of all types of rebars. It is found that the diameter of the tensile rebar of the second prediction is larger than in the tested specimen.

Table 5 Each actual diameter of rebar

	Rebar of compressive	Rebar of tensile	Stirrups
Actual diameter of rebar	D13	D13	D10

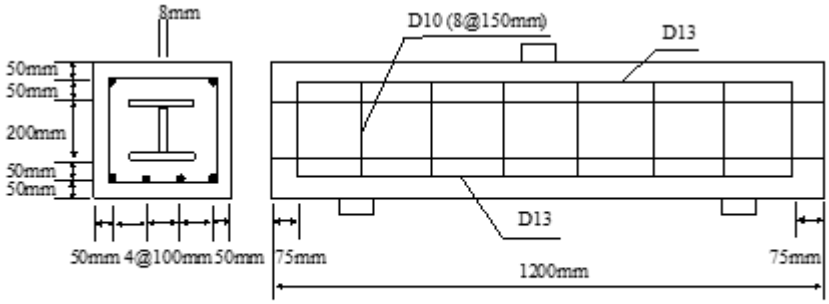

Fig.14 Actual design drawing of the specimen

6.2 Load-displacement curve

Fig.5.1 shows the load – displacement curves of the specimen at mid-span from FEA and experiment. In the experiment, the maximum load capacity is 1758 kN. This value is larger than value of FEA and hand calculation. Error is -9.4% for FEA and -26.1% of hand calculation, respectively. Therefore, FEA is reliable in the range. It could be considered that this gap may come from the error of the predicted material property of I-Beam structure. From the comparison between the predictions and actual design drawing, it is found that all diameters of rebar of actual structure are smaller than the predictions. However, the maximum loading capacity from experiment is larger than the load capacity from prediction. Therefore, this gap may come from the error of the material property of I-beam in the predicted specimen.

6.3 Procedure of cracking of Actual Structure and FEA

From section 5.1, the cracking procedure of the second prediction is got. Comparing to the actual structure, it is found that the second prediction reproduces the actual procedure of cracking reasonably well. As shown on the picture of the actual structure after damage (Fig.2), the specimen has two tensile micro cracking and two micro shear cracking. As shown on the picture of the actual specimen after failure (Fig.3), the shear cracking expands and leads to a shear failure finally. Comparing this experimental cracking procedure with the analytical cracking procedure using FEA (see Fig.13), it is found that the FEA using data from NDTs can provide an accurate prediction of the actual cracking procedure and damages.

6.4 Discussion from comparison

In this section, a comparison between the behaviors of the specimen from FEM and from experiment is conducted. As for the first prediction, it is very different from the actual specimen as no internal information from NDTs was provided until this prediction. This prediction has to be conducted by only referring other papers. Consequently, it was impossible to predict the internal structure or in other words whether the beam is an RC or SRC beam. In this prediction, the specimen was predicted as RC, however actual structure was SRC. In terms of the second prediction, the internal steel arrangement is predicted appropriately using the data from NDTs. The gap of the maximum load capacity between FEA of second prediction and the actual specimen is

163 kN which is only 9.4% of the experimental load capacity. This gap may be due to the difference of diameter of rebar, I-beam material property and concrete material property. However, the gap of maximum load capacity of between hand calculation of second prediction and the actual specimen is 460 kN, which is much larger than the FEA. Thus, the hand calculation has a room of improvement and can be used as a rough cross check of the FEA. Therefore, it would be demonstrated that the process of predicting the structure details by jointly using data from NDTs and referring related experiences and knowledge and then conducting FEA of the predicted structure can provide a structural performance evaluation with good accuracy.

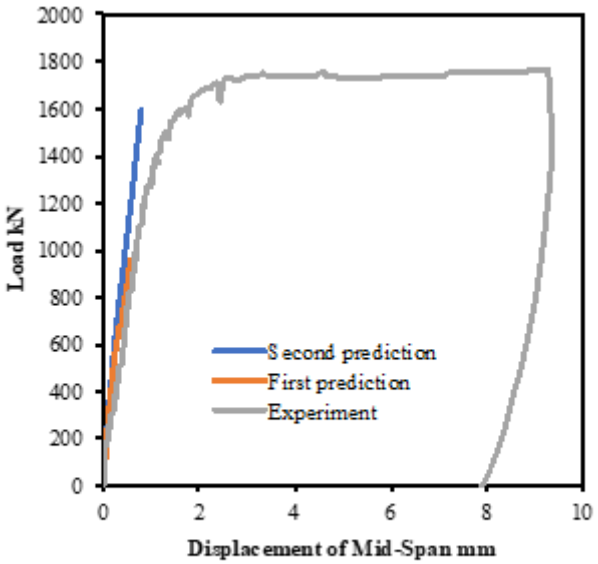

Fig. 15 Comparison of FEA and Experiment

7 Conclusion and Future Work

In this research, a process, namely blind performance evaluation, is conducted to predict and evaluate the structural performance of a beam using data from NDTs. The process can be described as follows. Firstly, a prediction of the details of the tested beam is conducted using date from inspection, measurement, and NDT technique together with referencing to related experiences and knowledge including standards, and academic article. Secondly, a nonlinear numerical analysis is conducted on the predicted structure based on FEM. Finally, the analytical behaviors of the structure are compared with the corresponding experimental behaviors to examine the proposed process for structural performance evaluation. Main findings can be concluded as follows:

1. The accuracy of the predictions depends greatly on the richness and completeness of the date from inspection, measurement, and NDTs. For example, the tested SRC beam was predicted incorrectly as an RC beam incorrectly with only pictures and dimensions and correctly as an SRC beam with additional data from NDTs. Besides, referencing to related experiences and knowledge can be a helpful supplementary for an appropriate prediction.
2. As the data from NDTs, such as material properties, may vary over wide ranges, it is of great significance to consider the effects of the obtained data on the behaviors of the structures.
3. For the SRC beam which is predicted using NDTs, a numerical analysis based on nonlinear FEA and a hand calculation based on empirical equations are conducted to predict the load capacity. Comparing with the experimental load capacity, it is found that the FEA can provide a good accuracy which is much higher than the hand calculation. This observation demonstrates the reliability and applicability of the proposed method and process. Nevertheless, the empirical equation can be a cross check of the FEA.
4. In addition, the experimental cracking procedure and shear failure mode are reproduced by the nonlinear FEA as well. Superior to the experiment and hand calculation, the FEA could provide a more detailed investigation of the structure.
5. In this research, the gap between FEA and the experiment may be from the modeling of the interface of rebar/concrete and I-beam/concrete. In this study, the materials or components are rigidly connected. As a future work, it may need to be improved.

References

1. Ministry of Land, Infrastructure, Transport and Tourism of Japan Homepage, https://www.mlit.go.jp/sogoseisaku/maintenance/02research/02_01.html, last accessed 2020/01/11
2. Muhammand S.: Finite Element Analysis of RC beams and slabs repaired with Ultra-high performance fiber reinforced concrete (UHPFRC). (2016)
3. MacGeregor, J.G.: Reinforced concrete mechanics and design. Prentice-Hall, Inc. Englewood Cliffs, NJ, (1992)
4. Kenji K.: Effect of shear span ratio on the fracture of deep beams. Journal of JSCE, 62(4), 798-814, (2006)
5. Yukihiro T.: Shear Strength of deep beams with sirups. Journal of JSCE, 2004(760), 29-44, (2004)
6. Hu, H.T., Lin, F.M., Jan, Y.Y.: Nonlinear finite element analysis of reinforced concrete beams strengthened by fiber-reinforced plastics. Journal of Composite Structures (63), 271-281, (2004).
7. Hu, H.T., Schnobrich W.C.: Nonlinear analysis of cracked reinforced concrete. ACI Structure Journal, 87(2), 102-118 (1999).